Hierarchical synchronization in complex networks with heterogeneous degrees

Changsong Zhou[a] and Jürgen Kurths
Institute of Physics, University of Potsdam PF 601553, 14415 Potsdam, Germany

(Received 12 August 2005; accepted 17 November 2005; published online 31 March 2006)

We study synchronization behavior in networks of coupled chaotic oscillators with heterogeneous connection degrees. Our focus is on regimes away from the complete synchronization state, when the coupling is not strong enough, when the oscillators are under the influence of noise or when the oscillators are nonidentical. We have found a hierarchical organization of the synchronization behavior with respect to the collective dynamics of the network. Oscillators with more connections (hubs) are synchronized more closely by the collective dynamics and constitute the dynamical core of the network. The numerical observation of this hierarchical synchronization is supported with an analysis based on a mean field approximation and the master stability function. © *2006 American Institute of Physics*. [DOI: 10.1063/1.2150381]

Complex networks are playing an increasing role in the understanding of complex systems. The analysis of various real-world complex systems using the approach of complex networks has uncovered general and important principles in the structure organization of realistic systems. In particular, many complex networks are scale-free, characterized by a heterogeneous power-law distribution of the degrees. A problem of fundamental importance is the impact of the network topology on the dynamics of the complex systems, which has been recently studied intensively in the context of synchronization of coupled oscillators. Many previous works have focused on the global synchronizability, i.e., the ability of the network to synchronize completely for fully identical oscillators. In this paper we consider more natural situations where the networks are not in the complete synchronization state, for example, when the coupling is not strong enough, when the oscillators are in the presence of noise or when the oscillators are nonidentical. We have shown that complex networks of chaotic oscillators display significant collective oscillations in such regimes. More interestingly, we have found that in networks with heterogeneous degrees, the individual oscillators have different levels of synchronization with respect to the collective oscillations and they exhibit a hierarchical dependence on the connection degrees. The behavior can be understood analytically based on a mean field approximation and the linear stability analysis. Our results demonstrate that, in the context of synchronization, hubs having large degrees play the leading role in the formation of the dynamical core, which is the main contributor to the collective dynamics of the network. In the future, it is interesting to study hierarchical synchronization in more realistic networks whose connection topology and connection strengths are time varying and the results could have meaningful applications in the dynamics of real-world complex systems, such as the human brain.

I. INTRODUCTION

Recent years have seen important progress in the study of complex systems from the view point of complex networks. The underlying idea is that many natural systems are composed of subelements with complicated interactions among them. The approach of complex network is to simplify the complex system by a graph, when representing the elements by the nodes of the graph and representing the interactions by the connections among the nodes. The resulting graphs often have a complex connection topology, i.e., they are complex networks.

The study of complex networks has revealed important and general organization principles in the topological structure of various real-world complex systems since the discoveries of the small-world[1] and the scale-free[2] properties. Small-world networks (SWNs) exhibit short average distance between nodes and high clustering,[1] while scale-free networks (SFNs) are characterized by having a power-law distribution of degree k (the number of connections per node),[2]

$$P(k) \sim k^{-\gamma}, \tag{1}$$

so that there does not exist a characteristic degree in the network. SFNs are featured by a statistical abundance of "hubs" with a very large number of connections k compared to the average degree value $K=\langle k \rangle$.

These seminal findings on complex networks have stimulated a great deal of research interest in a structure analysis of real-world complex systems from the viewpoint of network topology. It has been shown that both the small-world and the scale-free properties are universal in many real-world complex systems (cf. Refs. 3–7 and references therein).

[a]Electronic address: cszhou@agnld.uni-potsdam.de

 © 2006 American Institute of Physics

Downloaded 09 May 2006 to 141.89.176.14. Redistribution subject to AIP license or copyright, see http://chaos.aip.org/chaos/copyright.jsp

An issue of fundamental importance in the study of complex systems is the interplay between structure and dynamics, which has recently attracted a great deal of attention in the context of complex networks. The topology of the networks can have a systematic influence on their physical and dynamical properties, such as error and attack tolerance,[8] percolation transition,[9,10] epidemic spreading,[11–13] and cascading failures,[14] etc.

Synchronization of oscillators[15,16] is one of the widely studied dynamical behavior on complex networks. It has been shown that SWNs provide a better synchronization of coupled excitable neurons in the presence of external stimuli.[17] In pulse-coupled oscillators, synchronization becomes optimal in the small-world regime,[18] and it is degraded when the degree becomes more heterogeneous with increased randomness.[19,20] Investigation of phase oscillators[21] or circle maps[22] on SWNs has shown that when more and more shortcuts are created at larger rewiring probability, the transition to synchronization become easier.[21] These observations have shown that the ability of a network to synchronize is generally enhanced in SWNs compared to regular chains. This enhanced synchronization in SWNs has also been analyzed in the context of complete synchronization (CS) of identical chaotic systems.[23–26] Physically, this enhanced synchronizability was mainly attributed to the decreasing of the average network distance due to the shortcuts.

More recently, it has been shown that the ability of CS of identical chaotic oscillators also depends critically on the heterogeneity of the degree distribution.[27] In particular, random networks with strong heterogeneity in the degree distribution, such as SFNs, are more difficult to synchronize than random homogeneous networks,[27] despite the fact that heterogeneity reduces the average distance between the nodes.[28,29] The synchronizability in Refs. 23–27 is assessed based on the stability of the CS state using the spectral analysis of the network coupling matrix.

Many of these studies of CS have focused on the global synchronizability of the networks and its robustness with respect to removal of nodes[30] or edges.[26] In more realistic situations, CS of the whole network is not a natural state of the network's dynamics. Desynchronization happens often, for example, when the oscillators are subjected to perturbations due to noise or parameter drifts, or when the coupling strengths are not in the synchronization regime. The stability analysis of the CS state may not provide useful information about the dynamical behavior in such regimes. However, the networks may still display a significant collective dynamics and the dynamical pattern of the effective synchronization can be very interesting.

In this paper, we study the organization pattern of such effective synchronization in complex networks with heterogeneous degrees, i.e., in SFNs. We pay special attention to local synchronization behavior of oscillators with respect to the collective dynamics of the whole network in regimes outside the CS state. We show that the synchronization organization displays a hierarchical structure, which is generally observed when the CS state is perturbed by noise, when there is nonidentity in the oscillators or when the coupling strength is too weak to achieve CS. The hierarchical structure is manifested by the dependence of the synchronization properties on the connection degree k of the nodes. Interestingly, the stability analysis of the CS state can be adopted to provide an understanding of the hierarchical synchronization. The results of the SFNs are compared to random networks with homogeneous degrees which do not exhibit such hierarchical synchronization behavior.

The paper is organized as follows. In Sec. II we introduce the general model of dynamical systems and network structures considered here. The transition to CS and desynchronization by noise in identical oscillators are treated in Sec. III. We consider nonidentical oscillators in Sec. IV. Then possible extensions of these results to weighted networks and time-varying networks are discussed in Sec. V.

II. MODELS

A. Dynamical equations

Real networks are often growing and changing in their topological structures and likely to have different coupling strengths for different connections.[31] Global synchronization of time-varying networks has been studied recently in Refs. 31–34. Since our purpose is to study synchronization organization outside the complete synchronization regime due to heterogeneous degrees, we consider in the following the simpler case of time-invariant networks with uniform coupling strength for all the connections as in Refs. 25, 27, and 30. The dynamics of a such network of N coupled oscillators is described by

$$\dot{\mathbf{x}}_j = \tau_j \mathbf{F}(\mathbf{x}_j) + \frac{g}{K}\sum_{i=1}^{N} A_{ji}(\mathbf{x}_i - \mathbf{x}_j), \tag{2}$$

where $\mathbf{x}_j$ is the state of oscillator j and $\mathbf{F}=\mathbf{F}(\mathbf{x})$ governs the dynamics of each individual oscillator. The parameter τ_j controls the time scale of the oscillators. $A=(A_{ji})$ is the adjacency matrix of the underlying network of couplings, where $A_{ji}=1$ if there is a link from node i to node j, and 0 otherwise. Here we assume that the coupling is bidirectional so that $A_{ij}=A_{ji}$, i.e., A is symmetrical. The degree k_j of a node is $k_j=\Sigma_i^N A_{ji}$, and $K=(1/N)\Sigma_{j=1}^N k_j$ is the mean degree of the nodes in the network. g is the overall coupling strength. Note that in previous analysis of complete synchronization of identical oscillators,[25,27,30] more general output function $[\mathbf{H}(\mathbf{x}_i)-\mathbf{H}(\mathbf{x}_j)]$ (Refs. 25 and 27) or inner coupling matrix $\mathbf{C}(\mathbf{x}_i-\mathbf{x}_j)$ (Ref. 34) have been considered for the coupling term in Eq. (2), where too large coupling could lead to desynchronization of the networks. Here we avoid such complications by taking $\mathbf{H}(\mathbf{x})=\mathbf{x}$ (or $\mathbf{C}=\mathbf{I}$, the identity matrix). In this case, complete synchronization state is stable when the coupling strength g is larger than a certain threshold.

We analyze the paradigmatic Rössler chaotic oscillator $\mathbf{x}=(x,y,z)$,

$$\dot{x} = -0.97x - z, \tag{3}$$

$$\dot{y} = 0.97x + ay, \tag{4}$$

Downloaded 09 May 2006 to 141.89.176.14. Redistribution subject to AIP license or copyright, see http://chaos.aip.org/chaos/copyright.jsp

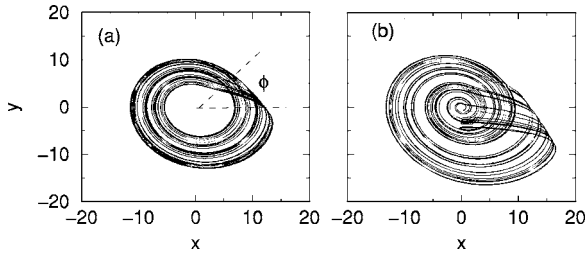

FIG. 1. Chaotic attractors of the Rössler oscillator in the phase coherent regime (a) and phase noncoherent regime (b).

$$\dot{z} = x(z - 8.5) + 0.4, \tag{5}$$

where the parameter a controls the coherence property of the phase dynamics of the oscillations. For example, at $a=0.15$, the oscillations are phase coherent [Fig. 1(a)] and at $a=0.25$, it is strongly phase noncoherent [Fig. 1(b)]. For the phase coherent oscillations, the trajectories rotate around a unique center and the phase can be defined simply by $\phi=\arctan(y/x)$.[35] Such a unique rotating center does not exist in the phase noncoherent oscillators, where the definition of phase is nontrivial.[36] With this system, we can study CS of identical oscillators as well as phase synchronization (PS) of nonidentical oscillators in Eq. (2).

B. Network models

Here we consider SFNs which are generated with the Barabási-Albert (BA) preferential attachment algorithm.[2] Starting with M fully connected nodes, at each time step a new node is added and connected to M existing nodes in the network, with the probability $\Pi_j \sim k_j$. The index of the nodes are sorted such that the degrees have a descending order, i.e., $k_1 \geqslant k_2 \geqslant, \ldots, k_N=M$ (Fig. 2). The resulting SFNs have a power-law degree distribution $P(k) \sim k^{-\gamma}$, with $\gamma=3$ (Fig. 2, inset) and the minimal degree $k_{\min}=M$, and the mean degree $K=2M$.

To demonstrate the impact of heterogeneous degrees, the synchronization behavior of the SFNs is compared to homogeneous networks (HNs) with the same mean degree K, where each node is connected randomly to exactly K other nodes in the network. The degree distribution of HNs is a delta function $P(k)=\delta(k-K)$. In this paper, we fix $N=1000$ and $K=10$.

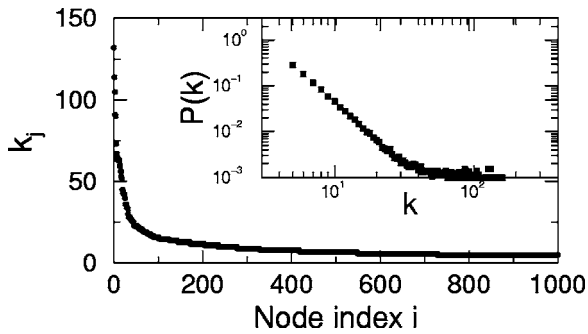

FIG. 2. Degree sequence k_j of a SFN with $N=1000$ nodes. The inset shows the power-law distribution $P(k) \sim k^{-\gamma}$, averaged over 50 realizations of the networks. The flat tail results from finite size effects.

III. IDENTICAL OSCILLATORS

In this section, we consider the case of transition to CS when the oscillators are identical, i.e., $\tau_1=\tau_2=\cdots=\tau_N=1$ in Eq. (2).

A. Linear stability

For identical oscillators, the completely synchronized state $\{\mathbf{x}_j(t)=\mathbf{s}(t), \forall j | \dot{\mathbf{s}}=\mathbf{F}(\mathbf{s})\}$ is an invariant solution of (2). Complete synchronization of the network requires that this solution is at least linearly stable.

The linear stability of this solution can be assessed in the framework of the master stability function.[25,37] Small perturbations of the synchronization state $\mathbf{s}$ are governed by the linear variational equations

$$\delta\dot{\mathbf{x}}_j = D\mathbf{F}(\mathbf{s})\,\delta\mathbf{x}_j - \frac{g}{K}\sum_{i=1}^{N} L_{ji}\delta\mathbf{x}_i, \quad j=1,\ldots,N, \tag{6}$$

where $D\mathbf{F}(\mathbf{s})$ is the Jacobian on $\mathbf{s}$ and $L=(L_{ji})$ is the Laplacian matrix, where $L_{ji}=-A_{ji}+\delta_{ji}k_j$. Note that the Laplacian matrix L has zero sum of the raws which corresponds to the invariance of the completely synchronized state $\mathbf{s}$. Equation (6) can be diagonalized into N decoupled blocks of the form

$$\dot{\eta}_j = \left(D\mathbf{F}(\mathbf{s}) - \frac{g}{K}\lambda_j\mathbf{I}\right)\eta_j, \quad j=1,\ldots,N, \tag{7}$$

where η_j is the eigenmode associated to the eigenvalue λ_j of the matrix L. Here $\lambda_1=0$, resulting from the manifold invariance, corresponds to the eigenmode parallel to the synchronization manifold, and the other $N-1$ eigenvalues λ_j represent the eigenmodes transverse to the synchronization manifold.

Note that all the eigenmodes have the same generic form

$$\dot{\eta} = [D\mathbf{F}(\mathbf{s}) - \epsilon\mathbf{I}]\eta, \tag{8}$$

except that $\epsilon=g\lambda_j/K$ are different by the eigenvalues λ_j. The largest Lyapunov exponent Λ of the generic mode (8) is a linear function of ϵ,

$$\Lambda(\epsilon) = \lambda_1^F - \epsilon, \tag{9}$$

where $\lambda_1^F>0$ is the largest Lyapunov exponent of the chaotic attractor of the isolated oscillator ($\epsilon=0$). So the jth mode is damped if $g\lambda_j/K>\lambda_1^F$ where $\Lambda<0$. The CS state is stable when the least stable mode η_2, associated with the minimal non-zero eigenvalue λ_2, is damped, namely when $g>g_c$, where $g_c=K\lambda_1^F/\lambda_2$.

When more general output function $\mathbf{H}(\mathbf{x})$ or inner-coupling matrix $\mathbf{C}$ is considered, Eqs. (7) and (8) will be changed accordingly, and the largest Lyapunov exponent Λ is usually negative in a finite interval of ϵ,[25,27,34] and complete synchronization may become impossible for large SFNs.[27]

B. Transition to synchronization

The transition to CS is shown in Fig. 3 for different networks and different chaotic regimes. Here we have plotted the average synchronization error $E=(1/N)\Sigma_{j=1}^{N}\Delta X_j$, where $\Delta X_j=\langle|x_j-X|\rangle_t$ is the time averaged difference be-

Downloaded 09 May 2006 to 141.89.176.14. Redistribution subject to AIP license or copyright, see http://chaos.aip.org/chaos/copyright.jsp

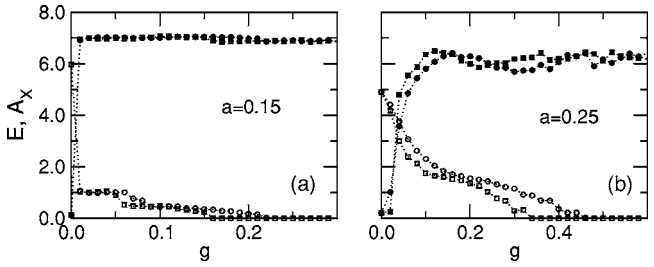

FIG. 3. Transition to CS in the SFN and the HN, indicated by the synchronization error E (squares) and the amplitude A_X of the mean field X (circles). The filled symbols are for the SFNs and the open symbols for the HNs. (a) Phase coherent oscillations at $a=0.15$. (b) Phase noncoherent oscillations at $a=0.25$. In both networks, $N=1000$ and $K=10$.

tween the oscillator x_i and the mean activity of the whole network, $X=(1/N)\Sigma_{j=1}^{N}x_j$. When CS is achieved at $g>g_c$, one has $E=0$ after a sufficiently long transient. We have also shown the oscillation amplitude A_X of the mean field X, calculated as the standard deviation of X over time. It is seen that the HN achieves CS at a critical coupling strength g_c smaller than that of the SFN having the same mean degree K. The synchronization error E decreases abruptly in the phase coherent regime when a very weak coupling suddenly synchronizes the phases of the chaotic oscillations, while E changes gradually in the phase noncoherent regime and achieves CS at larger g_c since the largest Lyapunov exponent λ_1^F is larger. In both networks, however, a collective oscillation with an amplitude A_X comparable to that of the completely synchronized state already emerges even for very weak coupling strengths g, both in the phase coherent and phase noncoherent regimes.

Now we look into the different behavior of the two networks during the transition to synchronization. For this purpose, we examine the synchronization difference ΔX_j of an individual oscillator with respect to the collective oscillations X of the whole network. It is seen in Fig. 4(a) that ΔX_j is almost the same for the nodes in the HN; in sharp contrast, it is strongly heterogeneous in the SFN and is negatively correlated with the degree k_j of the nodes. To get a clear dependence of ΔX on the degree k, we calculate the average value $\Delta X(k)$ among all nodes with degree k, i.e.,

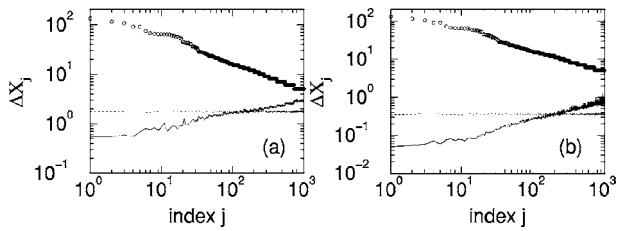

FIG. 4. Synchronization difference ΔX_j of the oscillators with respect to the global mean field X in the SFN (solid line) and HN (dotted line). The symbol (○) denotes the degree k_j of the nodes. Note the log-log scales of the plots. (a) When the coupling strength is weak ($g=0.1$) and (b) when the synchronized state ($g=0.5$) is perturbed by noise ($D=0.5$). Here the oscillations are phase noncoherent at $a=0.25$ and the behavior is very similar for phase coherent oscillations at $a=0.15$.

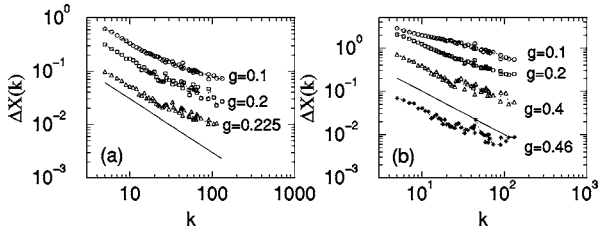

FIG. 5. The average values $\Delta X(k)$ as a function of k at various coupling strength g in the SFN. (a) Phase coherent regime $a=0.15$. (b) Phase noncoherent regime $a=0.25$. The solid line with slop -1 is plotted for reference.

$$\Delta X(k)=\frac{1}{N_k}\sum_{k_j=k}\Delta X_j, \tag{10}$$

where N_k is the number of nodes with degree $k_j=k$ in the SFN network. Now a pronounced dependence can be observed (Fig. 5). In the regime where the collective oscillation is significant with an amplitude comparable to that of the synchronized state ($g\gtrsim 0.05$), the dependence is characterized by a power-law scaling

$$\Delta X(k)\sim k^{-\alpha}, \tag{11}$$

with the exponent $\alpha\approx 1$ when the coupling strength g approaches to threshold g_c, both for the phase coherent [Fig. 5(a)] and phase noncoherent [Fig. 5(b)] regimes. These results demonstrate that in the SFNs, a small portion of nodes with large degrees synchronize more closely to the mean field X, while most of nodes with small degrees are still rather independent of X. A comparison of the results between the SFNs and the HNs in Fig. 4(a) shows that for the same coupling strength g, only about 20% of the nodes in the SFNs have the synchronization differences ΔX smaller than that of the HNs. In other words, in SFNs the pronounced collective oscillation X is only contributed by the hubs, while in HNs all the nodes have a significant contribution. This provides a physical reason that SFNs are more difficult to achieve CS than HNs.

C. Desynchronization by noise

When CS is obtained for $g>g_c$, desynchronization can be induced in the presence of noise. In our simulations, an independent noise $D\xi_i$ is added to the variable y of the oscillators in Eq. (2), where D represents the amplitude of the noise, and ξ_i follows the normal Gaussian distribution $N(0,1)$. As we can see from Fig. 4(b), the degree of desynchronization, again measured by ΔX, is rather homogeneous in the HN, while it also depends on the connection degree k in the SFN. The average value $\Delta X(k)$ again displays the power-law scaling as a function of k (Fig. 6), with $\alpha\approx 1$ independent of the noise level D if it is not too large.

So far we have shown that when the coupling strength is not strong enough to achieve CS or when the CS state is perturbed by external noise, the synchronization behavior in the SFNs having heterogeneous degrees displays a hierarchical structure. Nodes with larger degrees synchronize better and contribute more to the collective oscillations of the

Downloaded 09 May 2006 to 141.89.176.14. Redistribution subject to AIP license or copyright, see http://chaos.aip.org/chaos/copyright.jsp

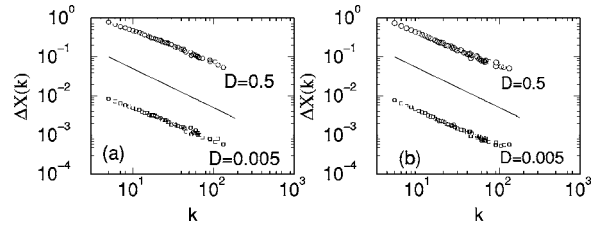

FIG. 6. The average values $\Delta X(k)$ as a function of k in the SFN at various noise levels D. (a) Phase coherent regime $a=0.15$ with the coupling strength $g=0.3$ in the CS region. (b) Phase noncoherent regime $a=0.25$ with $g=0.5$. The solid line with slop -1 is plotted for reference.

network. For a given mean degree K, the homogeneous network topology seems to be optimal for synchronization, since all the nodes have equally significant contributions.

D. Effective synchronization clusters

We have shown that the synchronization behavior of the individual oscillators in the SFNs is highly nonuniform. The nodes with large degrees are close to the mean field. As a result, the synchronization difference among them should be also relatively small. We can define an effective synchronization cluster for those oscillators which synchronize to each other within some threshold. For this purpose, we have calculated the pairwise synchronization difference $\Delta X_{ij}=\langle|x_i-x_j|\rangle_t$. A pair of oscillators $(i\neq j)$ is considered to be synchronized effectively when their synchronization difference is smaller than a threshold, $\Delta X_{ij}\leqslant\Delta_{\text{th}}$. Since the synchronization difference is heterogeneous, there is no unique choice of the threshold value Δ_{th}. What we can expect is that with smaller values of Δ_{th}, the size of the effective cluster is smaller. The effective synchronization clusters for different values of the threshold Δ_{th} are shown in Figs. 7(a) and 7(b). The same clusters are also represented in the space of degrees (k_i,k_j) in Figs. 7(c) and 7(d), respectively. Note that almost all the oscillators forming the clusters have a degree $k_j>k_{\text{th}}$ where k_{th} is the threshold degree satisfying $\Delta X(k_{\text{th}})=\Delta_{\text{th}}$; or correspondingly, the effective cluster is formed by nodes with $j<J_{\text{th}}$ where J_{th} is the mean index of nodes with degree $k_j=k_{\text{th}}$. The triangle shape of the effective clusters in Fig. 7 is well described by the relation $i+j\leqslant J_{\text{th}}$. Above the solid line $i+j=J_{\text{th}}$, those oscillators ($i\leqslant J_{\text{th}}$ and $j\leqslant J_{\text{th}}$) having large enough degrees, i.e., $k_i\geqslant k_{\text{th}}$ and $k_j\geqslant k_{\text{th}}$, are close to the mean field with $\Delta X_i\leqslant\Delta_{\text{th}}$ and $\Delta X_j\leqslant\Delta_{\text{th}}$, but the pairwise distance is large, $\Delta X_{ij}>\Delta_{\text{th}}$. These results demonstrate clearly that the hubs are the dynamical core of the networks.

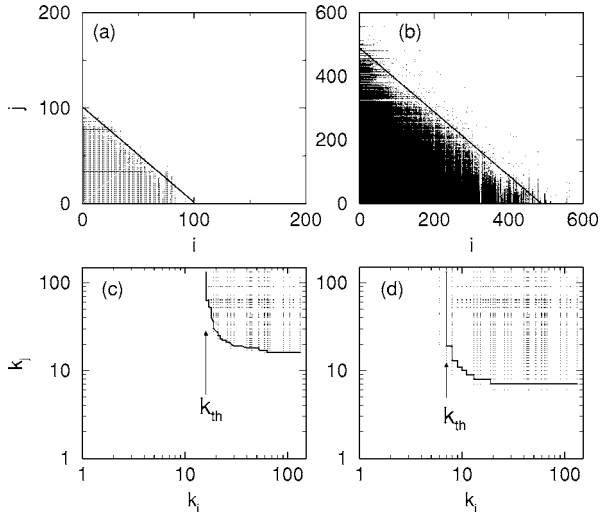

FIG. 7. The effective synchronization clusters in the synchronized network in the presence of noise ($a=0.25$, $g=0.5$, and $D=0.5$), represented simultaneously in the index space (i,j) [(a), (b)] and in the degree space (k_i,k_j) [(c), (d)]. A dot is plotted when $\Delta X_{ij}\leqslant\Delta_{\text{th}}$. (a) and (c) for the threshold value $\Delta_{\text{th}}=0.25$, and (b) and (d) for $\Delta_{\text{th}}=0.50$. The solid lines in (a) and (b) denote $i+j=J_{\text{th}}$ and are also plotted in (c) and (d) correspondingly. Note the different scales in (a) and (b) and the log-log scales in (c) and (d).

Some previous works have discussed cluster synchronization in complex networks.[38–41] There are two types of cluster formation in very sparse networks displaying tree-like structures.[38–40] One is self-organized cluster where the nodes within the cluster display internal connections. The other one is driven cluster, where the nodes of one cluster are driven by those of the others, but do not connect to other nodes of the same cluster. Cluster formation in this case is related to some symmetry in the networks[42] (e.g., a branch in the tree can form a self-organized cluster, and two branches connected to a common node can form driven clusters). Such symmetry vanishes with increasing connectivity in random networks, and a clear identification of these types of clusters becomes difficult, for example, for the networks considered here. We emphasize that the clusters in Fig. 7 are effective in the sense that there is still a synchronization difference among the oscillators even though they all synchronize to the mean field strongly.

E. Analysis of hierarchical synchronization

The hierarchical synchronization in SFNs when the coupling is not strong enough, or when there is noisy perturbation in the network, can be understood by the following analysis based on a mean-field approximation. Let $\bar{\mathbf{x}}_j=(1/k_j)\Sigma_{i=1}^{N}A_{ji}\mathbf{x}_i$ be the local mean field of all the neighbors connected to the oscillator j, Eq. (2) then can be rewritten as

$$\dot{\mathbf{x}}_j=\tau_j\mathbf{F}(\mathbf{x}_j)+\frac{gk_j}{K}(\bar{\mathbf{x}}_j-\mathbf{x}_j),\quad j=1,\ldots,N. \tag{12}$$

Since the network is random, for a node with the degree $k_j\gg 1$, the average signal it receives from its neighbors is sufficiently close to that of the whole network, i.e., the local mean field $\bar{\mathbf{x}}_j$ can be approximated by the global mean field $\mathbf{X}$ of the network, $\bar{\mathbf{x}}_i\approx\mathbf{X}$. And the system is approximated as

$$\dot{\mathbf{x}}_j=\tau_j\mathbf{F}(\mathbf{x}_j)+\frac{gk_j}{K}(\mathbf{X}-\mathbf{x}_j),\quad k_j\gg 1. \tag{13}$$

This approximation means that the oscillators are forced by a common signal $\mathbf{X}$, with the forcing strength being proportional to their degree k_j.

For identical oscillators ($\tau_j=1$), the linear variational equations of (13) read

Downloaded 09 May 2006 to 141.89.176.14. Redistribution subject to AIP license or copyright, see http://chaos.aip.org/chaos/copyright.jsp

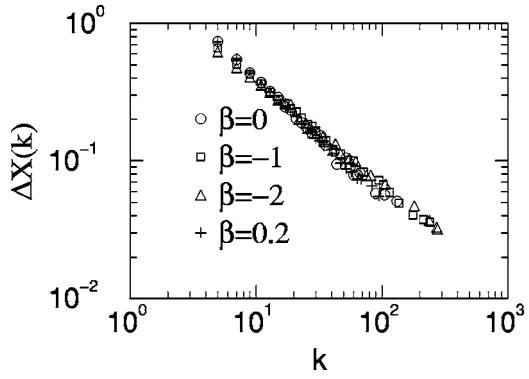

FIG. 8. $\Delta X(k)$ as a function of k for networks with different degree distributions (power law and exponential) due to different aging exponents β. The results obtained in the synchronization regime perturbed by noise ($a=0.25$, $g=0.5$, and $D=0.5$) in these different networks collapse into a single curve.

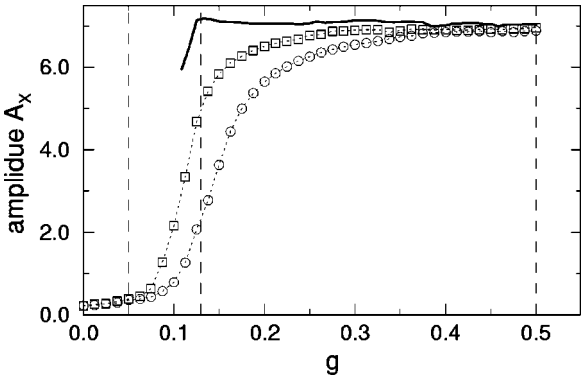

FIG. 9. The amplitude of the mean field as a function of the coupling strength g in the SFN (○) and HN (□). The solid line is the analytically obtained results [Eq. (20)] for globally coupled oscillators. The networks have the same mean degree $K=10$ and size $N=1000$.

$$\dot{\eta}_j = \left(D\mathbf{F}(\mathbf{X}) - \frac{g}{K} k_j \mathbf{I} \right) \eta_j, \quad k_j \gg 1, \tag{14}$$

which have the same form as (7), except that λ_j is replaced by k_j. According to Eq. (9), the largest Lyapunov exponent $\Lambda(k_j)$ of this linear equation is a function of k_j and becomes negative for $(g/K)k_j > \lambda_1^F$. For large k values satisfying $(g/K)k \gg \lambda_1^F$, we have $\Lambda(k) \approx -(g/K)k$.

Now suppose that the network is not completely synchronized, but perturbed slightly from it when the coupling strength g is below the threshold g_c, or when there is noise present in the system. For nodes with large degree k, so that $\Lambda(k) \approx -(g/K)k$ is sufficiently negative, the dynamics of the averaged synchronization difference $\Delta X(k)$ over large time scales can be expressed as

$$\frac{d}{dt}\Delta X(k) = \Lambda(k)\Delta X(k) + c, \tag{15}$$

where $c>0$ is a constant denoting the level of perturbation with respect to the CS state, which depends on the noise level D or the coupling strength g. From this we get the asymptotic result $\Delta X(k) = c/|\Lambda(k)|$, giving

$$\Delta X(k) \sim k^{-1}, \tag{16}$$

which explains qualitatively the numerically observed scaling in Figs. 5 and 6.

Note that the analysis does not use the knowledge of the degree distribution. The scaling in Eq. (16) should be general for random networks with different heterogeneous degree distributions. To show this, we have examined another growing model of SFNs proposed in Ref. 43. This model extended the BA model by taking into account the aging effects of the nodes. A node j is randomly selected to be connected to the new node with a probability Π_j which depends on the degree k_j and age τ_j of the corresponding node, i.e., $\Pi_j \sim k_j \tau_j^{-\beta}$, where β is the aging exponent controlling the aging effects. $\beta=0$ corresponds to the usual BA model,[2] which generate SFNs with a power-law degree distribution at $\gamma=3$. For the aging exponent $-\infty < \beta \leqslant 0$, this model generates SFNs with a power-law tail $P(k) \sim k^{-\gamma}$ and the scaling exponent in the interval $2 < \gamma \leqslant 3$,[43] as in most real SFNs. The degree distribution is exponential if $\beta > 0$.[43] As seen in Fig. 8, the scaling is the same for networks with different degree distributions at various β values.

For more general output function $\mathbf{H}(\mathbf{x})$ or inner-coupling matrix $\mathbf{C}$, the largest Lyapunov exponent Λ is usually negative in a finite interval of $\epsilon_1 < \epsilon < \epsilon_2$.[25,27,34] $\Lambda(\epsilon)$ decreases and then increases with ϵ. Equation (15) is still valid and the behavior reported above is general for relative weak coupling strengths g where $\Lambda(\epsilon)$ is in the decreasing regime. With larger g values, nodes with the largest degrees may enter into the increasing regime of $\Lambda(\epsilon)$ and the synchronization difference $\Delta X(k)$ increases with k again. $\Delta X(k)$ is minimal for some nodes with intermediate degrees, even though it may happen that there is no suitable values of g to achieve complete synchronization of the whole network. More details will presented elsewhere.

IV. NONIDENTICAL OSCILLATORS

Now we consider nonidentical oscillators by assuming that the time-scale parameters τ_j are heterogeneous, so that the oscillators have different mean oscillation frequencies Ω_j. In our simulations we use a uniform distribution of τ_j in an interval $[1-\Delta\tau, 1+\Delta\tau]$, with $\Delta\tau=0.1$. We focus on the phase coherent regime at $a=0.15$. In the phase noncoherent regimes, a phase variable could be defined based on the curvature of the oscillations[36] or use the recurrence plot.[44] The details are out of the scope of this paper, and will be studied elsewhere.

Let us first examine the collective oscillations in the network. Figure 9 shows the amplitude A_X of the mean field X as a function of the coupling strength g for the SFN and HN. It is seen that both networks generate a coherent collective oscillation when the coupling strength is larger than a critical value $g_{cr} \approx 0.08$. However, the SFN generates a weaker degree of collective synchronization as indicated by a smaller amplitude of the mean field.

Next we study in more detail the synchronization behavior in the weak, intermediate, and strong coupling regimes, indicated by the three vertical dashed lines in Fig. 9.

Downloaded 09 May 2006 to 141.89.176.14. Redistribution subject to AIP license or copyright, see http://chaos.aip.org/chaos/copyright.jsp

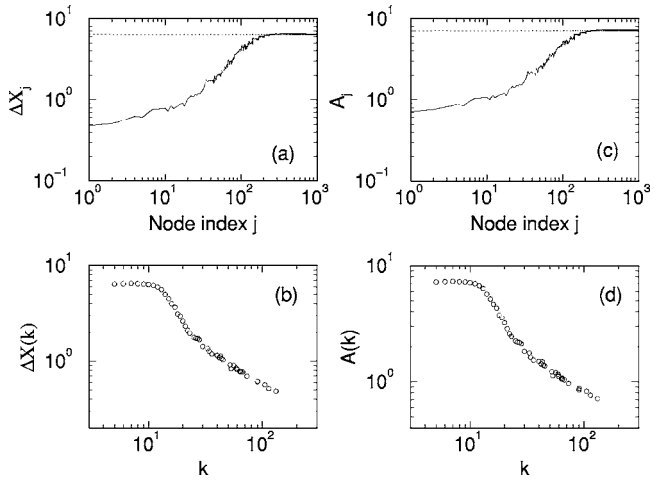

FIG. 10. (a) Synchronization difference ΔX_j of the oscillators with respect to the global mean field X in the SFN (solid line) and HN (dotted line). (b) The average values $\Delta X(k)$ as a function of k in the SFN. (c) and (d), as in (a) and (b), but for the oscillation amplitude A_j and the average value $A(k)$ of the oscillators. The results are averaged over 50 realizations of the random time-scale parameters τ_j. The coupling strength is $g=0.05$.

A. Weak coupling: Nonsynchronization regime

We start with the weak coupling regime with $g=0.05$. Here neither the HN nor the SFN displays significant collective oscillations. The frequencies of the oscillators are still distributed and the phases of the oscillators are not locked. However, interesting dynamical changes can be already expected in the SFN. Based on the mean field approximation in Eq. (13), even though the overall coupling strength g is still small, the oscillators with large degrees are already strongly forced by a common signal $\mathbf{X}$, which has only a very small amplitude in this weak coupling regime. These oscillators should somewhat synchronize to X. As shown in Figs. 10(a) and 10(b), oscillators with $k>10$ already display a degree of synchronization indicated by a decreasing ΔX for larger k, while all the oscillators in the HN are distant from X. A small distance of an oscillator j from X having an almost vanishing amplitude shows that the oscillation amplitude A_j of the oscillator is small. We have calculated A_j as the standard deviation of the time series x_j. We can see from Fig. 10(c) that A_j indeed display almost the same behavior of ΔX_j. This becomes even more evident when we compare the average value $A(k)$, in Fig. 10(d) with $\Delta X(k)$ in Fig. 10(b). The changes in the amplitudes can be understood as follows: taking $\mathbf{X}\approx\mathbf{X}_F$, from Eq. (13) one has

$$\dot{\mathbf{x}}_j = \tau_j \mathbf{F}(\mathbf{x}_j) - \frac{gk_j}{K}(\mathbf{x}_j - \mathbf{x}_F), \quad k_j \gg 1, \tag{17}$$

which shows that hubs are experiencing a strong negative self-feedback, so that the trajectory is stabilized at the originally unstable fixed point $\mathbf{x}_F$, but with some fluctuations due to small nonvanishing perturbations from the mean activity of the neighbors. The power-law tail in Fig. 10(d) can be qualitatively explained by the analysis in Sec. III E.

To summarize, in the weak coupling regime where even frequency and phase synchronization (PS) are not yet established, the heterogeneous SFN already displays a form of hierarchical synchronization expressed by the change in the oscillation amplitudes.

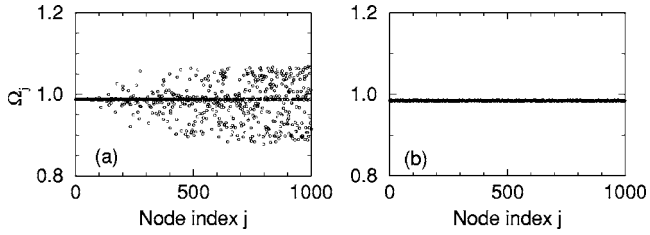

FIG. 11. The mean oscillation frequencies Ω_j of the oscillators in the SFN (a) and the HN (b) at the coupling strength $g=0.13$.

B. Intermediate coupling: Phase synchronization

Next we take an intermediate coupling strength $g=0.13$ where both networks are in the regime of transition to strong collective oscillations (Fig. 9). In this regime, frequency and PS become evident, while the absolute distance ΔX is still large. In Fig. 11 we show the mean oscillation frequencies Ω_j of the oscillators. In the SFN, about 70% of the nodes are locked to a common frequency $\Omega=0.99$, forming a frequency synchronization cluster. Note that most of the nodes with large degrees k_j are synchronized in frequency, while many nodes with small degrees are not locked yet. In the homogeneous network, on the contrary, the frequencies of all nodes are locked so that the network is globally synchronized in frequency. The nodes that are not frequency locked in the SFN, are largely uncorrelated with each other and they do not contribute to the collective oscillations, while all the nodes in the HN have a significant contribution; as a result, the amplitude of the collective oscillation is much smaller in the SFN, as seen in Fig. 12. Note also that the collective oscillations are periodic even though the oscillators are chaotic. Physically, this is due to the interplay between the parameter disorder and the coupling, which drives the system from the chaotic regime into the periodic regime. A more detailed and quantitative analysis of the bifurcation of the mean field will be discussed with a set of low-dimensional macroscopic equations in Sec. IV D.

Now we examine PS of the nodes with respect to $\mathbf{X}$. We measure PS by the time averaged order parameter,

$$R_j = \langle \sin(\Delta\phi_j)\rangle^2 + \langle \cos(\Delta\phi_j)\rangle^2, \tag{18}$$

where $\Delta\phi_j=\phi_j-\phi_X$ is the difference of the phases of an individual oscillator j and the mean field $\mathbf{X}$. Here the phases

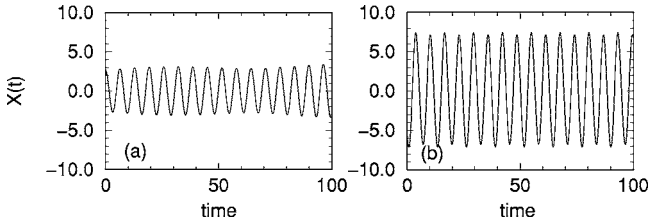

FIG. 12. Time series of the mean field X in the SFN (a) and HN (b) at the coupling strength $g=0.13$.

Downloaded 09 May 2006 to 141.89.176.14. Redistribution subject to AIP license or copyright, see http://chaos.aip.org/chaos/copyright.jsp

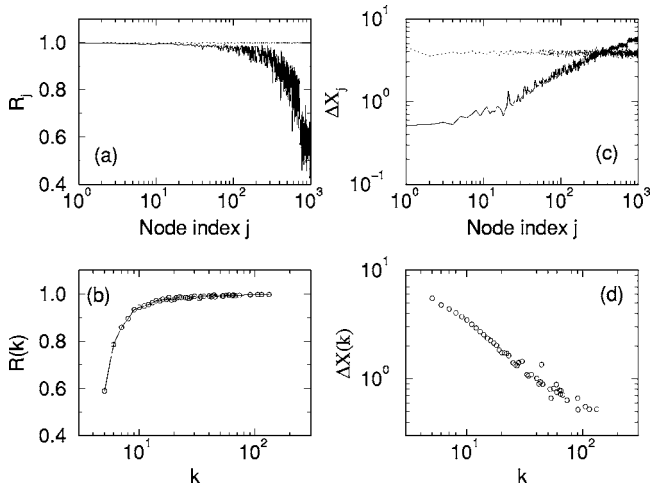

FIG. 13. (a) Phase synchronization order parameter R_j of node j with respect to the mean field $\mathbf{X}$ in the SFN (solid line) and HN (dotted line). (b) Average value $R(k)$ of nodes with degree k as a function of k in the heterogeneous network. (c),(d) as (a) and (b), but for the distance ΔX_j and its average value $\Delta X(k)$, respectively. The results are averaged over 50 realizations of random distribution of the time-scale parameter τ_j. The coupling strength is $g=0.13$.

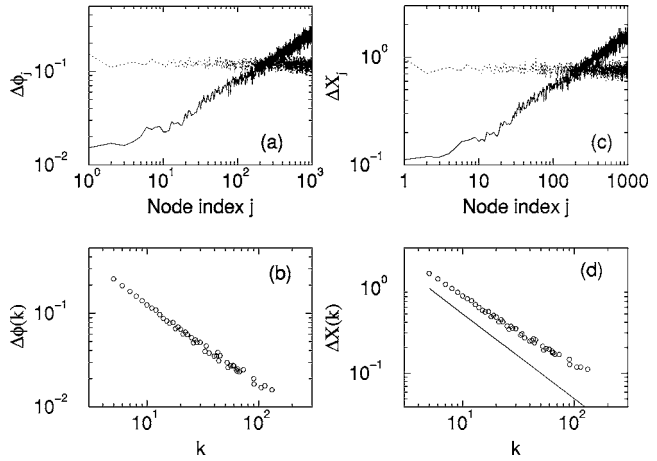

FIG. 14. (a) Averaged phase difference $\Delta\phi_j$ between a node j and the mean field X in the SFN (solid line) and HN (dotted line). (b) Average value $\Delta\phi(k)$ of nodes with degree k as a function of k in the SFN. (c),(d) as (a) and (b), but for the absolute difference ΔX_j and its average value $\Delta X(k)$, respectively. The solid line in (d) with slope $\alpha=1$ are plotted for reference. The results are averaged over 50 realizations of the random time scale parameters τ_j. The coupling strength is $g=0.5$.

are defined as $\phi_j=\arctan(y_j/x_j)$ and $\phi_X=\arctan(Y/X)$ for an individual oscillator j and the mean field, respectively. Note that $R_j\approx 0$ when there is no phase locking and $R_j\approx 1$ when the phases are locked with an almost constant phase difference. As consistent with Fig. 11, we find that $R_j=1$ for all the oscillators in the HN; while $R_j<1$ for many nodes with small degrees in the SFN [Fig. 13(a)]. To get a clear dependence of R on the degree k, again we calculate the average value $R(k)$ among all nodes with degree k. Now there is a more pronounced dependence between $R(k)$ and k [Fig. 13(b)].

We also calculate the absolute distances ΔX_j. They are not small on average in both networks in spite of phase synchronization [Fig. 13(c)], because phase locked oscillators may have significant phase differences. However, ΔX_j again display the hierarchical structure in the SFN [Fig. 13(d)]. The nodes with large degrees are not only locked in frequency, but also have a small phase differences. So in this regime, the hierarchical synchronization is manifested by different degree of frequency and phase locking.

C. Strong coupling: Almost complete synchronization

Now we consider the strong coupling regime where both networks have a large and saturated amplitude in the collective oscillations (Fig. 9).

We take $g=0.5$ at which the amplitude of X is almost the same for the two networks. The frequencies of all the oscillators are locked mutually as well as locked to the mean field; as a result, the phase synchronization order parameter is $R_j=1$ for all oscillators in both SFN and HN, i.e., the networks are globally phase synchronized. In the HN network, the phase difference $\Delta\phi_j$ between an oscillator and the mean field, averaged over time and over different realizations of random distribution of the time-scale parameters τ_j, is small and on average rather homogeneous for all the oscillators [Fig. 14(a)]. As a result, the oscillators are almost completely synchronized in the sense that $\Delta X\approx A_X\sin(\Delta\phi)\approx A_X\Delta\phi$ is also small and uniform on average [Fig. 14(c)]. In the SFN, however, many nodes with degree smaller than the mean value K is not as strongly connected to the mean field, and they have larger phase differences on average [Fig. 14(a)], as is shown evidently by the average value $\Delta\phi(k)$ over nodes with degree k [Fig. 14(b)]. Consequently, the synchronization difference ΔX_j is still heterogeneous [Fig. 14(c)] and $\Delta X(k)\sim k^{-\alpha}$ with $\alpha\approx 1$ [Fig. 14(d)]. This behavior can be understood qualitatively by the analysis of Eq. (15) in Sec. III E, where the perturbation level (constant c) now is due to the nonidentity in the time scale τ_j of the oscillators.

D. Analysis of the coherent regime of HN

We have seen that in the HN, the oscillators are almost completely synchronized at strong coupling strength, since the synchronization difference ΔX is small and uniform in the network. Now we carry out some analysis of the collective oscillation of the network based on the mean field approximation in Eq. (13). For the HN, there is $k_j=K$, and if $K\gg 1$ the mean field approximation (13) is equivalent to a globally coupled network,

$$\dot{\mathbf{x}}_j=\tau_j\mathbf{F}(\mathbf{x}_j)+g(\mathbf{X}-\mathbf{x}_j),\quad j=1,2,\ldots,N. \tag{19}$$

As the difference ΔX_j is uniformly small for all the oscillators, we can obtain the dynamical equations for the macroscopic variable $\mathbf{X}$. Let $\mathbf{x}_j=\mathbf{X}+\delta\mathbf{x}_j$. Expanding the system (19) with respect to $\mathbf{X}$ and neglecting the higher order terms $O(|\delta\mathbf{x}_j|^2)$ as proposed in, Ref. 45 we get the following low-dimensional macroscopic equations:

Downloaded 09 May 2006 to 141.89.176.14. Redistribution subject to AIP license or copyright, see http://chaos.aip.org/chaos/copyright.jsp

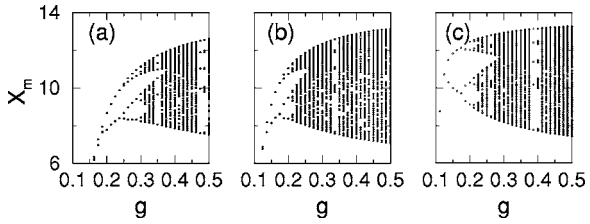

FIG. 15. Bifurcation diagram of the collective oscillations X with respect to the coupling strength g. The dots plotted are the local maxima X_m in the time series of X. (a) SFN, (b) HN, and (c) Macroscopic equations in Eq. (20).

$$\dot{\mathbf{X}} = \mathbf{F}(\mathbf{X}) + D\mathbf{F}(\mathbf{X})\mathbf{W},$$
$$\dot{\mathbf{W}} = \sigma_\tau^2 \mathbf{F}(\mathbf{X}) + D\mathbf{F}(\mathbf{X})\mathbf{W} - g\mathbf{W}, \tag{20}$$

where $D\mathbf{F}$ denotes the Jacobian matrix of $\mathbf{F}$. Here $\mathbf{W}=\langle(\tau_j-1)(\mathbf{x}_j-\mathbf{X})\rangle$ measures the dispersion in both the frequency and the state. σ_τ^2 is the variance of the distribution of τ_j.

The amplitude A_X of X obtained numerically from the macroscopic equations (20) is shown in Fig. 9 (solid line), which provides a good approximation for the HN over a broad range of coupling strength. The deviation becomes larger at smaller g where ΔX_j is not sufficiently small. In principle, the above analysis based on small value expansion is not applicable for the SFN in the same strong coupling regime, since the difference ΔX_j of many oscillators is not small. The difference is expected to vanish when g becomes sufficiently large so that almost complete synchronization is also achieved in the SFN.

Surprisingly, despite the large deviation of the macroscopic equations from the SFNs and from the HN at weak g, the bifurcations (period doubling to chaos) of the collective oscillations of the SFN and the HN are captured qualitatively (Fig. 15).

It is important to stress at this point that the sparsely connected networks ($K=10$ only) already generate a collective oscillation rather similar to that of globally coupled network described by the macroscopic equations in Eq. (20). This is of importance in real-world complex networks, such as neural networks, since sparse connections save a great deal of energy without degrading the essential function of the network.

V. CONCLUSION AND DISCUSSION

We have studied synchronization organization in complex networks out of the complete synchronization regime. A comparison between degree heterogeneous networks (SFNs) and degree homogeneous networks (HNs) has shown that heterogeneous degrees have significant effects on the organization of the effective synchronization of the networks. We have shown with numerical simulations and linear stability analysis that the synchronization properties of the nodes in the heterogeneous networks depend hierarchically on the degrees. The hubs having large degrees k are strongly influenced by the collective dynamics of the whole network and synchronize more closely to the collective dynamics. In other words, the hubs in the network form a dynamical core which is the main contributor to the collective dynamics of the whole network. In this way, we have demonstrated that the hubs in the topological structures of the networks are also the hubs of the functioning of the networks.

Here we have considered the impact of network topology on the synchronization organization by assuming that all the links are identical in strength. However, a more complete understanding of many realistic systems would require a characterization of networks beyond the topology. For example, different links can contribute differently. Many complex networks are actually weighted and display a highly heterogeneous distribution of both degrees and weights.[46–49] Examples include brain networks,[50,51] and airport networks,[46] which underlie the synchronization of epidemic outbreaks in different cities.[52,53] It has been observed that heterogeneity in the coupling strength can lead to desynchronization and localized instability in locally coupled regular networks of periodic oscillators[54] or in random networks of pulse-coupled oscillators.[55]

We have recently studied the synchronizability of weighted networks and shown that weighted coupling has significant effects beyond the network topology,[56–58] also see Ref. 59. Synchronization of complex networks is relevant in many real-world systems. For example, brain networks[50,51] display a hierarchy of oscillation and synchronization on various spatial and temporal scales. Heterogeneous weights in coupling strength are natural, for example, in city networks of coupled populations in the synchronization of epidemic outbreaks,[52,53] due to heterogeneous populations of the cities. In communication and other technological networks, the functioning of the system relies on the synchronization of interacting units.[60] The study of hierarchical synchronization organization in general weighted networks with heterogeneity both in the connection topology and in the connection strength represents an interesting and important research direction in the future and has important potential applications in real-world systems.

Real dynamical networks are often growing and changing in their connection topology and connection weights. Conditions and criteria for global synchronization in such time-varying networks have been discussed in Refs. 31–34. It is very interesting to investigate how effective synchronization patterns evolve in time due to the evolution of the structures in time-varying networks. So far, it is assumed that the structural changes in time-varying networks are independent of the oscillatory dynamics.[31–34] Our present interest is on self-organization of structures and dynamics due to the interplay between them.[61]

ACKNOWLEDGMENTS

The authors thank M. Matias and B. Blasius for helpful discussions. This work was supported by Grant No. SFB 555 (DFG) and the European Union through the Network of Excellence BioSim, Contract No. LSHB-CT-2004-005137.

[1] D. J. Watts and S. H. Strogatz, Nature (London) **393**, 440 (1998).
[2] A.-L. Barabási and R. Albert, Science **286**, 509 (1999).

Downloaded 09 May 2006 to 141.89.176.14. Redistribution subject to AIP license or copyright, see http://chaos.aip.org/chaos/copyright.jsp

[3]D. J. Watts, *Small Worlds* (Princeton University Press, Princeton, NJ, 1999).
[4]S. H. Strogatz, Nature (London) **410**, 268 (2001).
[5]R. Albert and A.-L. Barabási, Rev. Mod. Phys. **74**, 47 (2002).
[6]S. N. Dorogovtsev and J. F. F. Mendes, Adv. Phys. **51**, 1079 (2002).
[7]M. E. J. Newman, SIAM Rev. **45**, 167 (2003).
[8]R. Albert, H. Jeong, and A.-L. Barabási, Nature (London) **406**, 378 (2000).
[9]D. S. Callaway, M. E. J. Newman, S. H. Strogatz, and D. J. Watts, Phys. Rev. Lett. **85**, 5468 (2000).
[10]R. Chen, K. Erez, D. ben Avraham, and S. Havlin, Phys. Rev. Lett. **85**, 4626 (2000).
[11]R. Pastor-Satorras and A. Vespignani, Phys. Rev. Lett. **86**, 3200 (2001).
[12]R. M. May and A. L. Lloyd, Phys. Rev. E **64**, 066112 (2001).
[13]M. E. J. Newman, Phys. Rev. E **64**, 016128 (2002).
[14]A. E. Motter, Phys. Rev. Lett. **93**, 098701 (2004).
[15]S. Boccaletti, J. Kurths, G. Osipov, D. L. Valladares, and C. S. Zhou, Phys. Rep. **366**, 1 (2002).
[16]A. S. Pikovsky, M. G. Rosenblum, and J. Kurths, *Synchronization: A Universal Concept in Nonlinear Science* (Cambridge University Press, Cambridge, 2001).
[17]L. F. Lago-Fernández, R. Huerta, F. Corbacho, and J. A. Sigüenza, Phys. Rev. Lett. **84**, 2758 (2000).
[18]N. Masuda and K. Aihara, Biol. Cybern. **90**, 302 (2004).
[19]X. Guardiola, A. Diaz-Guilera, M. Llas, and C. J. Perez, Phys. Rev. E **62**, 5565 (2000).
[20]H. Hasegawa, Phys. Rev. E **70**, 066107 (2004).
[21]H. Hong, M. Y. Choi, and B. J. Kim, Phys. Rev. E **65**, 026139 (2002).
[22]A. M. Batista, S. E. D. Pinto, R. L. Viana, and S. R. Lopes, Physica A **322**, 118 (2003).
[23]P. M. Gade and C. K. Hu, Phys. Rev. E **62**, 6409 (2000).
[24]J. Jost and M. P. Joy, Phys. Rev. E **65**, 016201 (2001).
[25]M. Barahona and L. M. Pecora, Phys. Rev. Lett. **89**, 054101 (2002).
[26]J. Lu, X. Yu, G. Chen, and D. Cheng, IEEE Trans. Circuits Syst., I: Fundam. Theory Appl. **51**, 787 (2004).
[27]T. Nishikawa, A. E. Motter, Y.-C. Lai, and F. C. Hoppensteadt, Phys. Rev. Lett. **91**, 014101 (2003).
[28]F. Chung and L. Lu, Proc. Natl. Acad. Sci. U.S.A. **99**, 15879 (2002).
[29]R. Cohen and S. Havlin, Phys. Rev. Lett. **90**, 058701 (2003).
[30]X. Wang and G. Chen, IEEE Trans. Circuits Syst., I: Fundam. Theory Appl. **49**, 52 (2002).
[31]J. Lu, X. Yu, and G. Chen, Physica A **334**, 281 (2004).
[32]S. Sinha, Phys. Rev. E **66**, 016209 (2002).
[33]I. Belykh, V. Belykh, and M. Hasler, Physica D **195**, 188 (2004).
[34]J. Lu and G. Chen, IEEE Trans. Autom. Control **50**, 842 (2005).
[35]M. G. Rosenblum, A. S. Pikovsky, and J. Kurths, Phys. Rev. Lett. **76**, 1804 (1996).
[36]G. V. Osipov, B. Hu, C. S. Zhou, M. V. Ivanchenko, and J. Kurths, Phys. Rev. Lett. **91**, 024101 (2003).
[37]L. M. Pecora and T. L. Carroll, Phys. Rev. Lett. **80**, 2109 (1998).
[38]S. Jalan and R. E. Amritkar, Phys. Rev. Lett. **90**, 014101 (2003).
[39]S. Jalan and R. E. Amritkar, Physica A **321**, 220 (2003).
[40]S. Jalan and R. E. Amritkar, Physica A **346**, 13 (2005).
[41]L. G. Morelli, H. A. Cerdeira, and D. H. Zanette, Eur. Phys. J. B **43**, 243 (2005).
[42]I. Stewart, Nature (London) **427**, 601 (2004).
[43]S. N. Dorogovtsev and J. F. F. Mendes, Phys. Rev. E **62**, 1842 (2000).
[44]M. C. Romano, M. Thiel, J. Kurths, I. Z. Kiss, and J. Hudson, Europhys. Lett. **71**, 466 (2005).
[45]S. De Monte, F. d'Ovidio, and E. Mosekilde, Phys. Rev. Lett. **90**, 054102 (2003).
[46]A. Barrat, M. Barthélemy, R. Pastor-Satorras, and A. Vespignani, Proc. Natl. Acad. Sci. U.S.A. **101**, 3747 (2004).
[47]S. H. Yook, H. Jeong, A.-L. Barabási, and Y. Tu, Phys. Rev. Lett. **86**, 5835 (2001).
[48]M. E. J. Newman, Phys. Rev. E **64**, 016132 (2001).
[49]L. A. Braunstein, S. V. Buldyrev, R. Cohen, S. Havlin, and H. E. Stanley, Phys. Rev. Lett. **91**, 168701 (2003).
[50]D. J. Felleman and D. C. Van Essen, Cereb. Cortex **1**, 1 (1991).
[51]J. W. Scannell, G. A. P. C. Burns, C. C. Hilgetag, M. A. O'eil, and M. P. Yong, Cereb. Cortex **9**, 277 (1999).
[52]B. T. Grenfell, O. N. Bjornstad, and J. Kappey, Nature (London) **414**, 716 (2001).
[53]N. C. Grassly, C. Fraser, and G. P. Garnett, Nature (London) **433**, 417 (2005).
[54]J. G. Restrepo, E. Ott, and B. R. Hunt, Phys. Rev. Lett. **93**, 114101 (2004).
[55]M. Denker, M. Timme, M. Diesmann, F. Wolf, and T. Geisel, Phys. Rev. Lett. **92**, 074103 (2004).
[56]A. E. Motter, C. S. Zhou, and J. Kurths, Europhys. Lett. **69**, 334 (2005).
[57]A. E. Motter, C. S. Zhou, and J. Kurths, Phys. Rev. E **71**, 016116 (2005).
[58]A. E. Motter, C. S. Zhou, and J. Kurths, AIP Conf. Proc. **776**, 201 (2005).
[59]M. Chavez, D.-U. Hwang, A. Amann, H. G. E. Hentschel, and S. Boccaletti, Phys. Rev. Lett. **94**, 218701 (2005).
[60]G. Korniss, M. A. Novotny, H. Guclu, Z. Toroczkai, and P. A. Rikvold, Science **299**, 677 (2003).
[61]C. S. Zhou and J. Kurths (unpublished).

Downloaded 09 May 2006 to 141.89.176.14. Redistribution subject to AIP license or copyright, see http://chaos.aip.org/chaos/copyright.jsp